Dynamic Modeling and Control of Flexible Space Structures

Jang-Soo Chae*
Graduate Student, Department of Mechanical Engineering, Ajou University, Paldal-Gu, Suwon, Kyungki-Do 442-749, Korea
Tae-Won Park
Professor, Department of Mechanical Engineering, Ajou University, Paldal-Gu, Suwon, Kyungki-Do 442-749, Korea

This paper presents a global mode modeling of space structures and a control scheme from the practical point of view. Since the size of the satellite has become bigger and the accuracy of attitude control more strictly required, it is necessary to consider the structural flexibility of the spacecraft. Although it is well known that the finite element (FE) model can accurately model the flexibility of the satellite, there are associated problems : FE model has the system matrix with high order and does not provide any physical insights, and is available only after all structural features have been decided. Therefore, it is almost impossible to design attitude and orbit controller using FE model unless the structural features are in place. In order to deal with this problem, the control design scheme with the global mode (GM) model is suggested. This paper describes a flexible structure modeling and three-axis controller design process and demonstrates the adequate performance of the design with respect to the maneuverability by applying it to a large flexible spacecraft model.

Key Words : FSS (Flexible Space Structure), Vibration Suppression, Reaction Wheel, GM (Global Mode) Model, ACS (Attitude Control System), Flexibility

1. Introduction

In the past, satellites were small in size and required minimal electrical power since they performed simple missions in space. But the satellites and other space structures today have very complex missions and hence they may need more electric power. As a result, the solar panels of the today's common satellites are required to be large in order to generate sufficient electrical power.

In the previons works, the satellite systems were generally considered to be rigid bodies (Iwens, 1982 ; Howley, 1996 ; Bang and Lho, 2001), but since their solar panels have flexibility, it is necessary to consider flexibility effects when modeling the satellite's dynamic system and designing the attitude and orbit controller (Hughes, 1972, 1987 ; Wie et al., 1984).

It is known that the performance of the attitude and orbit control system (AOCS) is degraded by structural flexibility. Hughes (1972) and Ryan (1990) found that flexible appendage such as the solar array of a satellite has a very small damping ratio in the low frequency region and can be modeled by a sum of the number of flexible modes. Because the natural frequencies of the modes are widely distributed and some of them may be located near the attitude control bandwidth, they can be stimulated by control torque force (Balas, 1982).

Moreover, some of the expected disturbances can easily excite low frequency vibration on the bus system. Such vibration will degrade the per-

* Corresponding Author,
E-mail : jschae@koreaaero.com
TEL : +82-42-939-3571; **FAX** : +82-42-939-3500
Graduate Student, Department of Mechanical Engineering, Ajou University, Paldal-Gu, Suwon, Kyungki-Do 442-749, Korea. (Manuscript **Received** January 29, 2003; **Revised** September 29, 2003)

formance of the satellite system that needs to maintain specific shape or attitude with high accuracy. Junkins et al.(1993) investigated the reason why the flexibility in vibration control should be considered in controller design. Wie and Liu (1993) investigated the solar array vibration on telescope pointing jitter using classical and H_∞ control design.

In general, the finite element method is used in modeling flexible space structures. It is well known that the FE model is accurate, but it has some defects as follows: (1) It has high order system matrix, (2) not easy to get the physical insights due to design changes, and (3) can be constructed only after all structural features have been decided. So it is impossible to pre-design an attitude controller using the FE model. Therefore it is desired to consider some other practical methods to model the flexibility of the satellite. This paper presents global mode analysis methods that includes flexibility of appendage of spacecraft. For design convenience, two or three flexible modes have strong effects on attitude/orbit and the control subsystem is generally chosen in modeling. The modeling process is presented first and the resultant flexible model is applied to pre-built rigid body attitude controller. After analysis of the flexibility effect on control performance, the controller is reinforced with the first order filters and the improved performance of the controller design is shown by simulation results. Classical control has been addressed in previous studies for spacecraft control using the reaction wheel (Li et al., 1996).

2. Modeling by Global Mode Analysis

2.1 Equations of motion

In this section, we will consider only one axis rotational motion of a spacecraft with the assumption of no cross coupling effects between the axes. It will be shown in section 5 that this assumption is not restrictive.

The geometrical modeling of the satellite with a complex large solar panel using beam model is shown in Fig. 1, We will use some variables, x

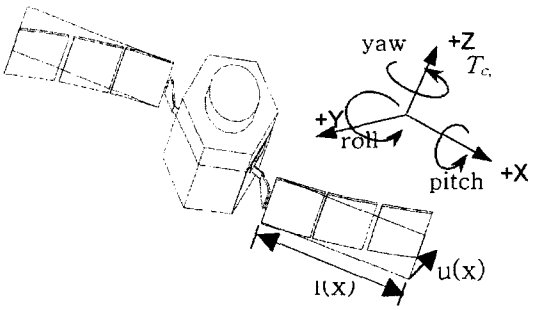

Fig. 1 Discrete model consisting of a rigid body and flexible beam

for span wise variable, $u(x)$ for the beam deflection, and a is outer radius of the hub along the undeformed appendage axis, θ_r is the hub angle, l is the length of the flexible structure (beam), and T_c is control torque produced by the reaction wheel on the rigid body. Here, we have neglected radial deformations and the nonlinear radial velocity correction required to rigorously enforce zero elongation of the deformed appendage.

The flexible structure is assumed to be slender. To formulate the problem, we shall make use of the extended Hamilton's principle given by the variational statement (Meirovitch, 1990),

$$\int_{t_1}^{t_2}\delta(T-V)\,dt+\int_{t_1}^{t_2}\delta W_{nc}dt=0 \tag{1}$$

In Eq. (1), T is the kinetic energy, V is the potential energy, δW_{nc} is the virtual work of the system, $\delta(\ )$ is the variational operator and t is time variable. The partial differential equations of motion for the elementary case of beam flexure using the Euler-Bernoulli beam theory neglecting axial-force effects, shear effects and rotary inertia is

$$\begin{aligned}&\partial^2u(x,\,t)/\partial t^2+(EI/\rho A)\,\partial^4u(x,\,t)/\partial x^4=\ddot{\theta}_r(x)\\&I_r\ddot{\theta}_r-2\rho A\int_a^{a+l}x(\partial^2u(x,\,t)/\partial t^2)\,dx=T_c\end{aligned} \tag{2}$$

Where the flexural stiffness is EI, system moment of inertia is I_r, and the mass per unit area is ρA, all of which are taken to be constants along the beam length in Eq. (2). In order to find the natural frequencies and corresponding mode shapes, consider the homogeneous version of the

first part of Eq. (2).

$$\partial^2 u(x, t)/\partial t^2+(EI/\rho A)\,\partial^4 u(x, t)/\partial x^4=0 \quad (3)$$

One form of solution of Eq. (3) can be represented by

$$u(x, t)=\psi(x)\,T(t) \quad (4)$$

Eq. (4) can be interpreted as cantilever motion with a constant shape $\psi(x)$ in which the amplitude varies with time according to $T(t)$. And $T(t)$ can be written as

$$T(t)=A\sin(\omega_n t)+B\cos(\omega_n t) \quad (5)$$

where

$$\omega_n^2=(\beta l)_n^4 EI/ml^2$$

In Eq. (5), the constants A and B depend on the initial velocity and displacement conditions. The shape function, $\psi(x)$, has the general form given by

$$\begin{aligned}\psi(\xi)=&c_1\cosh(\beta l\xi)+c_2\sinh(\beta l\xi)\\&+c_3\cos(\beta l\xi)+c_4\sin(\beta l\xi)\end{aligned} \quad (6)$$

The constants, c_n, $n=1, \cdots, 4$ in Eq. (6) represent the shape and amplitude of the cantilever beam vibration. These constants are evaluated by consideration of the boundary conditions of the cantilever beam.

2.2 Global mode analysis

The global mode analysis is a method that is distinct from the other analysis methods such as cantilever modal analysis (Marcel, 1997). Global mode (GM) model analysis generates total flexible system directly. In order to get the global mode shape, we take the system from free vibration when we allow the rotational motion of the center-body in absence of the control torque. We take the drive system equation in the presence of the control torque and body motion from the cantilever model. This method is more practical than the cantilever mode in controller design. Wie and Liu (1993) studied the flexibility of solar array, which has the most significant interaction with the spacecraft. They introduced the flexibility of structures to spacecraft using a second order transfer function.

The equation of motion of the spacecraft can be expressed in dimensionless variables, η and ξ, that are written as follows.

$$\partial^2\eta/\partial t^2+(EI/ml^3)\,\partial^4\eta/\partial\xi^4=\ddot{\theta}_r(\xi+a/l) \quad (7)$$

$$I_r\ddot{\theta}_r-2ml^2\int_0^1(\xi+a/l)\,(\partial^2\eta/\partial t^2)\,d\xi=T_C \quad (8)$$

where,

$$x=l\xi+a,\ u=\eta l,\ m=rho^*Al$$

In this paper, we are concerned with the symmetric and anti-symmetric modes involving center-body rotation, which are the more significant modes because the anti-symmetric modes are important in view of the attitude control. We can take normalized displacement function as

$$\eta=\sum_{n=1}^{\infty}\phi_n(\xi)\cos(\Omega_n t) \quad (9)$$

and rigid rotation angle as

$$\theta_r=\sum_{n=1}^{\infty}b_n\cos(\Omega_n t) \quad (10)$$

Substituting Eqs. (7) and (8) into Eqs. (9) and (10), we obtain

$$\begin{aligned}&\partial^4\phi_n(\xi)/\partial\xi^4-(\beta l)_n^4\phi_n(\xi)\\&=(\beta l)_n^4(\xi+a/l)\,b_n\end{aligned} \quad (11)$$

$$2ml^2\int_0^1(\xi+a/l)\,\phi_n(\xi)\,d\xi=I_r b_n \quad (12)$$

In Eq. (11), $(\beta l)_n$ is given by

$$(\beta l)_n^4=ml^3\Omega_n^2/EI \quad (13)$$

and $\phi_n(\xi)$ contains an arbitrary constant.

In order to obtain the mode shape and the frequency equation, apply the boundary conditions at both ends of the beam. We obtain the frequency equation as follows.

$$\begin{aligned}&2ml^2\{2(\beta l)^2[\tan(\beta l)+\tanh(\beta l)]\\&\quad+2\beta l[\tan(\beta l)+\tanh(\beta l)]\\&\quad+[\tan(\beta l)-\tanh(\beta l)]\}\\&=-J_r(\beta l)^3[1+\sec(\beta l)\operatorname{sech}(\beta l)]\end{aligned} \quad (14)$$

Eg. (14) is a transcendental equation in βl and must be solved numerically for eigenvalues β from which we can readily obtain frequencies (Meirovitch, 1967). J_r denotes the center body moment of inertia.

In the presence of the control torque, the deformation function can be represented as

$$\eta(\xi, t)=\sum_{n=1}^{\infty}\phi_n(\xi)\,q_n(t) \tag{15}$$

By eliminating the rotation angle θ_r in Eqs. (7) and (8), we obtain

$$\begin{aligned}&\partial^2\eta/\partial t^2-(2ml^2/I_r)(\xi+a/l)\int_0^1(\xi+a/l)\,\partial^2\eta/\partial t^2 d\xi\\&+(EI/ml^3)\,\partial^4\eta/\partial\xi^4\\&=(\xi+a/l)\,Tc/I_r\end{aligned} \tag{16}$$

From Eqs. (7), (8), and (15), we obtain

$$\begin{aligned}&\sum_{n=1}^{\infty}\{[\phi_n-(2ml^2/j_r)(\xi+a/l)\int_0^1(\xi+a/l)\,\phi_n d\xi\\&\quad+(EI/ml^3)](\ddot{q}_n+\Omega_n^2 q_n)\}\\&=(\xi+a/l)\,Tc/I_r\end{aligned} \tag{17}$$

By applying Eq. (12), Eq. (17) becomes

$$\begin{aligned}&\sum_{n=1}^{\infty}\{[\phi_n-b_n(\xi+a/l)(\ddot{q}_n+\Omega_n^2 q_n)]\}\\&=(\xi+a/l)\,Tc/I_r\end{aligned} \tag{18}$$

Now, by multiplying $\phi_j(\xi)$ and integrating over the range $\xi=0$ to $\xi=1$ to obtain the system dynamic equation after applying the boundary conditions and the orthogonality conditions, Eq. (18) can be written as

$$(\ddot{q}_n+\Omega_n^2 q_n)=A_n Tc/I_r \tag{19}$$

where A_n is given by

$$A_n=\frac{b_n}{(2ml^2/I_r)\int_0^1\phi_n^2 d\xi-b_n^2} \tag{20}$$

To facilitate the analysis of Eq. (19), we take its Laplace transformation in terms of $\theta_r(s)$ —s is the Laplace transform variable— and obtain

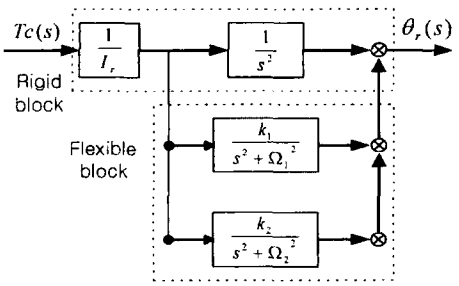

Fig. 2 Simplified global mode model (GMM) block diagram

$$\theta_r(s)=\left(\frac{Tc(s)}{I_r s^2}\right)\left\{1+s^2\sum_{n=1}^{\infty}\frac{k_n}{s^2+\Omega_n^2}\right\} \tag{21}$$

where the modal gain k_n for the global mode is given by

$$k_n=\frac{2ml^2/I_r\left[\int_0^1(\xi+a/l)\,\phi_n d\xi\right]^2}{\int_0^1\phi_n^2 d\xi-2ml^2/I_r\left[\int_0^1(\xi+a/l)\,\phi_n d\xi\right]^2} \tag{22}$$

The block diagram of Eq. (21) is shown in Fig. 2. In this paper, we consider only the first (bending mode) and the second mode (anti-symmetric bending mode) for the controlles design porpose since they are more important than the torsional mode from the attitude control point of view. The present method can be easily extended by just adding additional modes.

3. Evaluation of GM and FE Model

In this section, the GM model and the FE model are numerically evaluated, and bode plots of single axis control loop using the resultant models are presented. The overall control loop can be represented as in Fig. 3. The flexible structure model of Fig. 3 is substituted with the GM model and the FE model to compare the resulting frequency response though the GM model is not as accurate as the FE model, it gives good resemblance of the satellite's dynamics. So, the GM model can be regarded as a good model for designing the controller of a large flexible structure.

Generally, the FE analysis is performed after most of design key parameters are fixed. Since the a dynamic characteristics of two models are

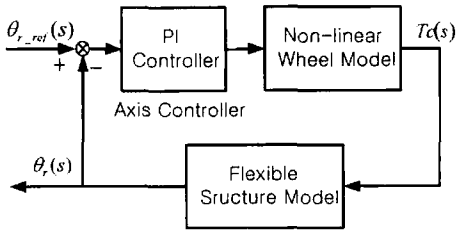

Fig. 3 Simplified control loop block diagram without filter

simular, we can perform the design of controller and a numerical simulation on the GM model to suppress the vibration.

3.1 Global mode model

Table 1 shows variables and their values for the GM model analysis. In this paper, only the first two flexible modes are modeled but it can be extended to include additional modes if more accurate model is desired.

Table 1 Coefficients of global mode model (GMM)

Parameters	Values	Unit
A	0.435	m
l	1.500	m
I_r	307.50	kg·m^2
Ω_1	3.0787	radian/seconds
Ω_2	4.5867	radian/seconds

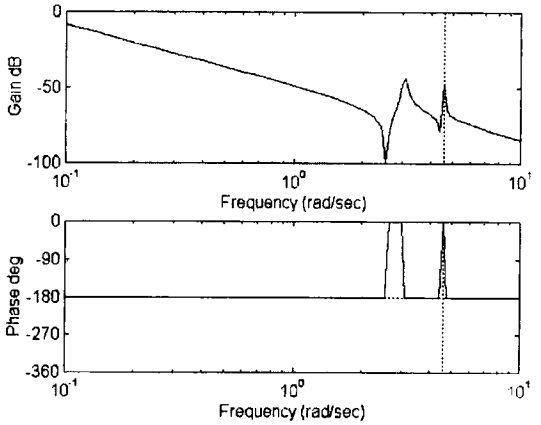

Fig. 4(a) Bode magnitude plot of the loop transfer function of rooll maneuver for the global mode model (GMM)

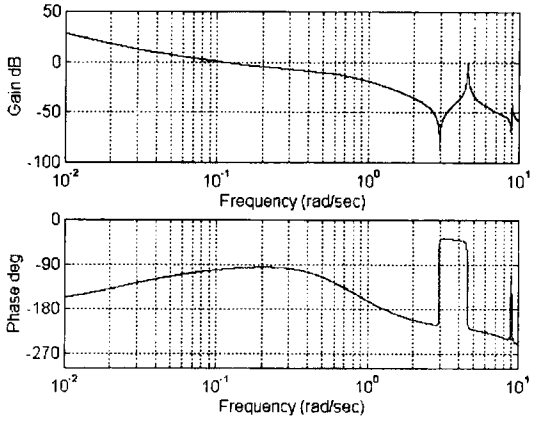

Fig. 4(b) Bode magnitude plot of the loop transfer function of rooll maneuver for the finite element model (FEM)

The transfer function can be built by getting the gain of k_1 and k_2 from Eq. (22) by applying the values of Table 1. The calculated values of these gains are $k_1=0.4312$ and $k_2=0.1003$ for the roll axis, whereas the other gains for the pitch and yaw axes are negligible compared to the roll axis. A bode plot of the GM model with two flexible modes is shown in Figs. 4(a) and 4(b). Two surges appear clearly around the first and second flexible modes and their frequencies are 0.49 Hz and 0.73 Hz. The more exact model can be obtained by considering the higher order modes, but it is thought that two flexible mode model can provide a suifable model for the controller design.

3.2 Finite element model

The FE model is derived from MSC/NASTRAN finite element model after key design parameters hare been fixed. For the finite element analysis, the moment of inertia for the flexible structure is shown in Table 5. And, it takes a state space representation in order to fit into an attitude control loop. The dynamics of this block are represented as follows

$$A=\begin{bmatrix} 0 & I \\ -\omega_n^2 & -2\zeta\omega_n \end{bmatrix},\ B=\begin{bmatrix} 0 \\ \psi_{wheel\ x,y,z}^T \end{bmatrix} \quad (23)$$
$$C=[\ \psi_{Gyro}\ 0\ ],\ D=[0]$$

The A of Eq. (23) is 40×40 matrix and has the natural frequency ω_n (see Table 2), and the modal damping ratio, $\zeta=0.002$. The dimension of the input matrix B is 40×3 and that of the output matrix C is 3×40 and I represents the unit matrix. The dimension of the matrix was determined along with the MSC/NASTRAN results. The important results of MSC/NASTRAN analysis and vibration test data for controller design are shown in Table 2. The first 6 modes are rigid body motion (3 translations and 3 rotations). The others are the first bending mode and the second anti-symmetric bending mode, and the torsional mode. From the FE results, bode plot

Table 2 Modal descriptions for flexible structure

Mode number	Frequency	Description
1-6	—	Rigid Body Motion
7	0.49 Hz	1st Bending Motion
8	0.73 Hz	2nd bending Motion
9	0.94 Hz	Torsion Motion

is easily drawn as in Fig. 4(b). Two surges around the frequencies of 0.49 Hz and 0.73 Hz represent the first and second bending modes, respectively.

Remarks 3-1: The same phenomenon in which two surges are caused by two flexible modes can be observed in Fig. 4(a) and Fig. 4(b) at the same frequencies. Therefore, though both plots are not exactly identical, it is easily known that the frequency characteristics of the GM model provide enough resemblance to those of the FE model for designing the axis controller.

Remarks 3-2: Although the FE model can represent flexible system accurately, it cannot be obtained until all the structural features are decided. So, it is desirable to use the GM model before the FE model is decided. Both modeling methods are not direct and do not require two-step methods.

4. Spacecraft Attitude Control Logics

The controller will also utilizes quaternion feedback where the quarternions are associated with an eigenaxis rotation about an Euler axis with unit vector $e=(e_1, e_2, e_3)$. Quaternion feedback control scheme has been proposed for the three-axis large maneuvers, where global stability is guaranteed (Wie et al., 1989). The quaternions are

$$q_1=e_1\sin(\phi/2) \tag{24}$$

$$q_2=e_2\sin(\phi/2) \tag{25}$$

$$q_3=e_3\sin(\phi/2) \tag{26}$$

$$q_4=\cos(\phi/2) \tag{27}$$

where ϕ is the angle about the Euler axis rotation angle and $e_{1,2,3}$ are direction cosines of the Euler axis with respect to the inertial refenence frame. An important relationship to note is shown in Eq. (28).

$$q_2^2+q_2^2+q_3^2+q_4^2=1 \tag{28}$$

By reducing the differential equations, the quaternion vector is denoted as $q=[q_1\ q_2\ q_3]^T$ and q_4 is the generated angle necessary for the implementation of the controller.

$$\dot{q}=-\frac{1}{2}\omega\times q+\frac{1}{2}q_4\omega \tag{29}$$

$$\dot{q}_4=-\frac{1}{2}\omega^T q \tag{30}$$

The control torque is defined as

$$T_C=-K_pq_e-K_d\omega-K_i\int q_e dt \tag{31}$$

where T_c is the control torque and disturbance torque. Thd control torque input can be assumed to be known for subsequent steering logic design and wheel momentum. Classical *PID* controller gains, K_p, K_d and K_i, were achieved for each axis considering the system stability, settling time, steady state error and bandwidth, etc. To avoid stimulating the natural frequency of the flexible body, the controller in reaction wheel has bandwidth 10 times larger than the flexural body frequency of 0.02 Hz

5. Filter Design

It is shown that without the isolation and attenuation of the flexible modes, the attitude of the spacecraft can be destabilized by the interaction with a large flexible mode. A low pass filter is shown to be an effective way to provide the necessary attenuation and isolate the control from the flexible mode

The top-level requirements imposed on the controller design are shown as follows

(1) Bandwidth of the axis controller is 0.02 Hz and 0.2 Hz for motor controller.

(2) Overshoot should be less than 20% and shorter than 200 seconds in settling time.

(3) Gain margin of over 10dB and phase margin of over 30 degrees.

Table 3 gives the performance results when the GM model is used as the flexible satellite model in the control loop shown in Fig. 5. It is important to note that for the roll axis, the gain margin is too small to satisfy the design requirements. In general, the dynamics of flexible structures in the low frequency region makes a resonance at bending frequencies with limiting control bandwidth. To eliminate this effect, two kinds of filter (1^{st} and 2^{nd} order low pass filter) are considered and it is shown that the first order filter giver by Eqs. (32) and (33) is sufficient

$$G_{in}(s)=\frac{\alpha}{s+\alpha} \tag{32}$$

$$G_{out}(s)=\frac{\beta}{s+\beta} \tag{33}$$

$\alpha=5$ is chosen in accordance with the inner loop's bandwidth, and $\beta=7$ in accordance with the outer loop's bandwidth. The frequency of the first asymmetric array flapping and its effects are examined. To examine the effects of the low pass filter, stability performance is obtained using the control loop shown in Fig. 5(see Table 3). The gain margin of the roll axis controller is increased from 3.547dB to 16.12dB through filtering. It is generally known that by adding the low pass filter, the top-level requirements of the attitude controller are satisfied. In the case of pitch or yaw axis controller that does not meet the requirements, a new filter design will be needed for that axis. Comparing the results of Figs. 8(a) and 8 (c) give insight into the nature of the filter influence.

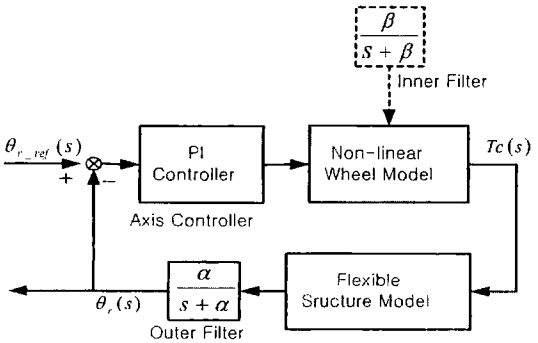

Fig. 5 Block diagram of control loop with low pass filters

6. Numerical Results

To perform the time domain analysis and three axes simulation, a pre-built three axes simulation loop is used. The objectives of the simulation are to verify a cross coupling between the axes and to demonstrate the filter's capability for eliminating the unfavorable effects. The roll axis gain,

Table 3 Stability performance of three-axis control loop without filter in flexible structures

Gain and Phase Margin (without filter)	
Roll	Gain : 3.547 dB@0.7233 Hz Phase : 58.23 deg@0.0176 Hz
Pitch	Gain : 21.04 dB@0.2032 Hz Phase : 82.17 deg@0.2142 Hz
Yaw	Gain : 20.07 dB@0.1701 Hz Phase : 81.64 deg@0.0165 Hz
Motor controller	Gain : 12 dB@0.3303 Hz Phase : 40 deg@0.1130 Hz

Table 4 Stability performance of three-axis control loop with filter in flexible structures

Gain and Phase Margin (without filter)	
Roll	Gain : 16.12 dB@0.1302 Hz Phase : 76.07 deg@0.0176 Hz
Pitch	Gain : 14.21 dB@0.1300 Hz Phase : 76.79 deg@0.0212 Hz
Yaw	Gain : 16.38 dB@0.1305 Hz Phase : 77.48 deg@0.0164 Hz
Motor controller	Gain : 10.53 dB@0.3285 Hz Phase : 38.84 deg@0.1146 Hz

Table 5 Parameters for dynamic modeling and controller design with flexible structures

Moments of Inertia	Values (kg·m²)		
I_{xx}, I_{xy}, I_{xz}	307.50	2.08	−180
I_{yx}, I_{yy}, I_{yz}	2.08	148.32	−8.30
I_{zx}, I_{xy}, I_{zz}	−1.80	−8.30	216.10
time delay	0.25 sec		
Gains	**Values**		
Roll	$K_p=32$, $K_i=0.69$		
pitch	$K_p=14$, $K_i=0.35$		
yaw	$K_p=20$, $K_i=0.40$		

in the absence of the filter, do not meet the margin of top-level requirements as shown in Table 3.

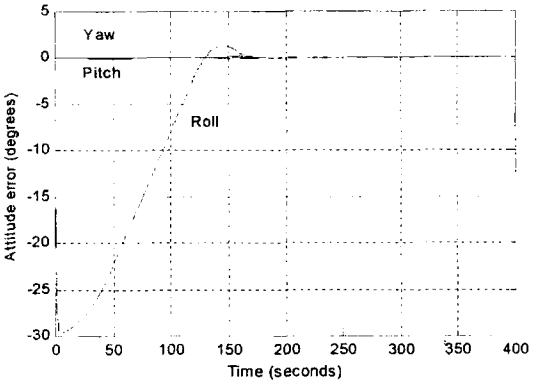

Fig. 6(a) Attitude error (the roll, pitch and yaw axis) with flexibility from the simulation results of KOMPSAT-1

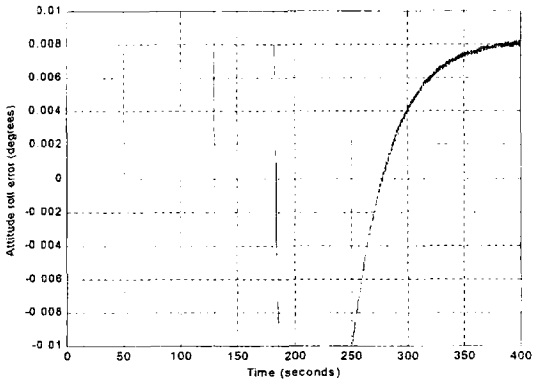

Fig. 6(b) Attitude roll error with flexibility from the simulation results of KOMPSAT-1

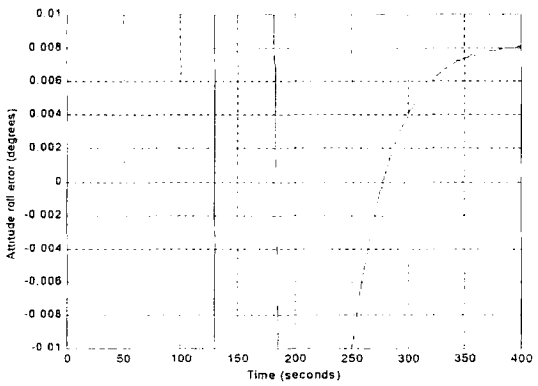

Fig. 6(c) Attitude roll error without flexibility from the simulation results of KOMPSAT-1

Table 4 shows the stability margin for the GM model with the filter, which demonstrates the effectiveness of the filter in improing the performance.

Figure 6 shows the simulation step response of 30 degrees attitude command input on roll axis. In Fig. 6, there are cross coupling effects in the pitch and yaw responses and they are caused by the flexibility of the satellite. Figs. 6(b) and 6(c) show the effects the flexable structures such as solar array on spacecraft during roll maneuver.

Compared to the rigid body model, the response for the flexible body takes more than 30 seconds to settle down. It is evident that the disturbance may excite the flexible mode. Comparing the results of Figs. 6(a), 6(b) and 6(c) with 7, we can observe the characteristics of the flexibility effects. The simulation of the global mode (GM) model and on-orbit model shows that the settling time is 350 sec. It means that the wheel momentum is generated to perform this rotation and subsequently goes diminished to zero when attitude errors become zero. For a rigid satellite, no such cross coupling effects are observed. The magnitude of the cross coupling effects is about 0.05 degrees about pitch and yaw axes. Figure 7 shows that a large roll maneuver response from of in-orbit telemetry data KOMPSAT (KOrea Multi Purpose SATellite at the a altitude of 685 Km. We find that the simulation model result shows a very good correspondence with

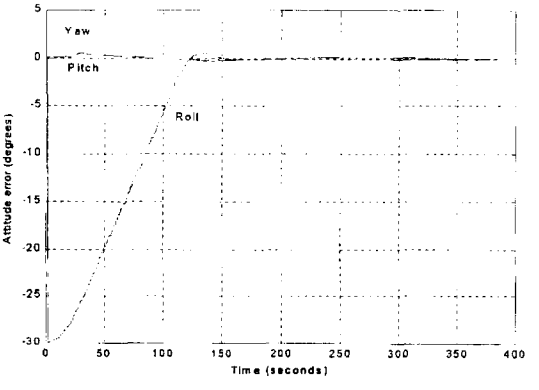

Fig. 7 Attitude error (the roll, pitch and yaw axis) from on orbit AOCS telemetry data of KOMPSAT-1

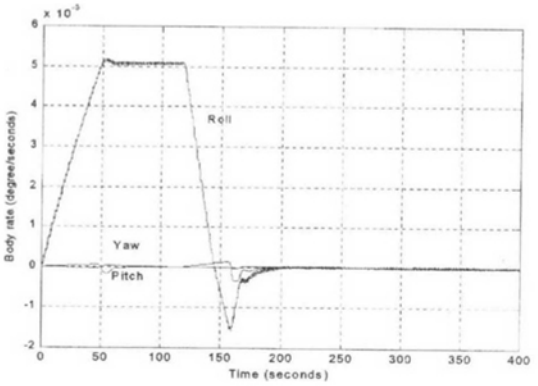

Fig. 8(a) Spacecraft body rates for a displacement of q=[0.0362 0 0] with flexibility on the reaction wheel control

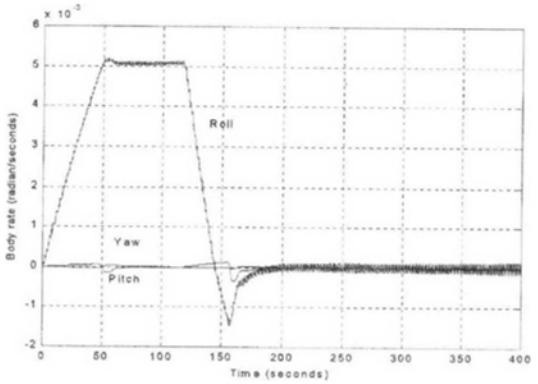

Fig. 8(b) Unfiltered spacecraft body rates with flexibility on the reaction wheel control for science mode

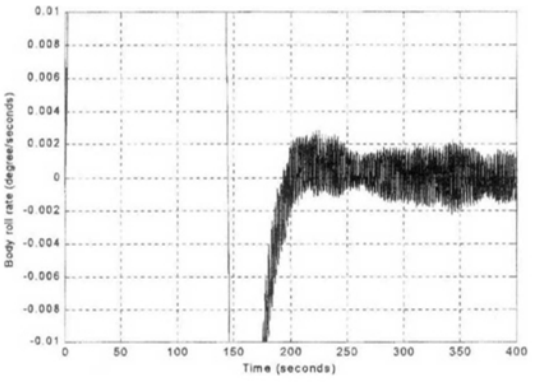

Fig. 8(c) Spacecraft roll rates with flexibility on the reaction wheel control for science mode

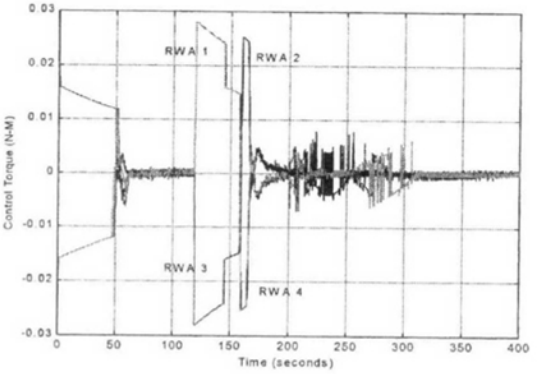

Fig. 9 Reaction wheel torque for a spacecraft on the spacecraft control

the in-orbit telemetry data. However, about the overshoot and settling time, some differences exist between the simulation model and in-orbit model. It has limitations and differences compared with the in-orbit environment. The spacecraft body rotation rates for the external disturbance T_d=1.0 e-4 Nm is shown in Figs. 8(a) and 8(c) given an initial quaternion displacement of q=[0.0362 0 0]. A 350 second slew duration is used here to represent a typical precision pointing maneuver for science mode. In other words, the wheel generates momentum to compensate for the attitude error between the initial quaternion and the command quaternion so that the satellite can adjust its attitude to the desired one. Figures 8(a), 8(b) show the effects of the low pass filter that provides the attenuation and isolate the control system from the flexible mode. Fig. 9 shows a good convergence characteristic of the error quaternions and it clearly demonstrates that the wheel speed limitation and torque capability are within the range of the specification of the reaction wheel.

7. Conclusions

In this paper an attitude control problem of a large flexible spacecraft is studied, with a free-free flexible model having a reaction wheel as an actuator and gyro sensor. It is shown that the GM is an effective model for attitude controller design for space structures with a large flexible mode.

The performance of the proposed controller is slightly altered by adding flexibility to the rigid satellite model. The performance enhancement by inconporating low pass filters is shown by the improvement in the gain margin and phase margin. It shows that low pass filters are effective in providing a necessary attenuation and in isolating the control system from the appendage flexible mode.

The numerical simulation results showed that the cross-coupling of the axes are negligible in the presence of filters. And the controller designed using the GM model is applicable to the FE model. The results of this paper provide a basis for systematic constant feedback gain solution of large angle flexible spacecraft rotational maneuvers in which flexibility needs to be considered. The designed controllers for a large flexible model are verified by numerical simulations with in-orbit satellite measurement data.

References

Balas, M. J., 1982, "Trends in Large Space Structures Control Theory: Fondest Hopes, Wildest Dreams," *IEEE Transaction on Automatic Control*, Vol. 27, No. 3, pp. 552~535.

Bang, H. and Lho, Y., 2001, "Sliding Mode Control for Spacecraft Containing Rotating Wheels," AIAA

Guidance, Navigation, and Control Conference & Exhibt(2001-4213).

Howley, B., 1996, "Genetic Programming of Spacecraft Attitude Maneuvers Under Reaction Wheel Control," AIAA Guidance, Navigation, and Control Conference(96-3849).

Hughes, P. C., 1987, "Spacecraft Attitude Dynamics," John Wiley & Sons.

Marcel, J., 1997, Spacecraft Dynamics and Control, Cambridge University Press.

Hughes, P. C., 1972, "Attitude Dynamics of a Three-Axis Stabilized Satellite with a Large Flexible Solar Array," *Journal of the Astronautical Sciences*, Vol. 20, No. 3.

Iwens, R. P., 1982, *Basic Spacecraft Attitude Control Tools*.

Junkins J. L. and Kim, Y., 1993, *Introduction to Dynamics and Control of Flexible Structure*, AIAA Education Series, Published by American Institute Of Aeronautics and Astronautics, Washington, D.C.

Li, X., Throckmorton, A. J. and Boka, J. B, 1996, "Stability Analysis on Earth Observing System AM-1 Spacecraft Earth Acquistion," AIAA Guidance, Navigation, and Control Conference(96-3827).

Likins, P. W., 1979, "The New Generation of Dynamics Interaction Problems," *Journal of Astroautical Sciences*, Vol. XXVII, No. 2.

Meirovitch, L., 1990, Dynamics and Control of Structures, Wiley, New York.

Meirovitch, L., 1967, Analytical Methods in Vibrations, Macmillan, New York.

Ryan, R. R., 1990, "Simulation of Actively Controlled Spacecraft with Flexible Appendages," *Journal of Guidance and Control*, Vol. 13, No. 4, pp. 691~702.

Wie, B. and Liu Q., 1993, "Classical and Robust Control Redesign for the Hubble Space Telescope," *Journal of Guidance Control and Dynamics*, Vol. 6, No. 6, pp. 1069~1077.

Wie, B. and Plescia, C. T., 1984, "Attitude Stablization of Flexible Spacecraft During Station Keeping Maneuvers," *J. of Guidance and Control*, Vol. 7, No. 4, pp. 62~68.

Wie, B., Gonzales, M., 1992, "Control Synthesis for Flexible Space Structure Excited by Persitent Disturbance," *Journal of Guidance and Control, Dynamics*, Vol. 15, No. 1, pp. 73~80.